Light Metals 2014
Edited by: John Grandfield
TMS (The Minerals, Metals & Materials Society), 2014

Light Metals 2014

CAST SHOP FOR ALUMINUM PRODUCTION

Grain Refinement/Solidification

SESSION CHAIR
Dmitry Eskin
Brunel University
Uxbridge, United Kingdom

Light Metals 2014
Edited by: John Grandfield
TMS (The Minerals, Metals & Materials Society), 2014

GRAIN REFINEMENT OF ALUMINIUM ALLOYS: RECENT DEVELOPMENTS IN PREDICTING THE AS-CAST GRAIN SIZE OF ALLOYS REFINED BY Al-Ti-B MASTER ALLOYS

Mark A. Easton[1], David H. StJohn[2], Arvind Prasad[2]
[1]School of Aerospace, Mechanical and Manufacturing Engineering, RMIT, Bundoora, Victoria, Australia 3083
[2]Centre for Advanced Materials Processing and Manufacturing, School of Mechanical and Mining Engineering, The University of Queensland, St Lucia, Australia 4072

Keywords: Aluminium alloys, grain refinement, Interdependence model

Abstract

This paper presents the results of recent research on the grain refinement of aluminium alloys. There has been considerable development in our understanding of the mechanisms controlling grain refinement over the last decade and these will be briefly described. In particular, the Interdependence Model has clearly explained the interdependence between the growth of grains and the nucleation potency of refining particles in causing a wave of nucleation events throughout a casting. This interaction determines the final as-cast grain size. A key factor identified by this research is the formation of a nucleation-free zone in front of a growing grain that prevents nucleation up to the point where a critical amount of constitutional supercooling is established allowing the next nucleation event to occur. Thus, the grain size is determined by the size of the nucleation-free zone and the distance to the next most potent particle. The Interdependence Model can, therefore, be used to predict grain size changes with composition and nucleant particle density. In this paper the Interdependence Model is used to develop equations for predicting the grain size of aluminium alloys when refined by Al-Ti-B master alloys. The performance of Al-5Ti-1B and Al-3Ti-1B master alloys are compared in the light of the Model.

Introduction

The CAST CRC solidification group began to study the grain refinement of aluminium alloys in the late 1990s with our first paper being published in 1996 on the importance of solute in promoting the nucleation of α-Al by TiB_2 [1]. Since then we have continued to develop our understanding of the mechanisms controlling grain refinement not just of aluminium alloys [2-6] but also of magnesium [7-11] and titanium alloys [12-14]. In all cases the role of solute is important and an equiaxed zone is not able to form, except in special circumstances, if no solute is present such as in pure metals. Therefore, the critical issue in understanding grain refinement is the way in which solute and the inoculant or native particles interact. This approach eventually led to the publication of the Interdependence Theory in 2011 which takes both of these factors into account [15, 16].

In this paper we briefly present the key elements of the Interdependence Theory and the most recent research that has been carried out to validate the Interdependence Model (the equation that embodies the Interdependence Theory). We then consider the practical application of the Model to the grain refinement of aluminium alloys.

The Interdependence Model

The Interdependence Theory shows that the formation of an equiaxed microstructure throughout a casting is facilitated by Constitutional Supercooling (CS) which generates sufficient undercooling to nucleate the next most potent particle present in the alloy melt [15, 16]. In the case of aluminium alloys the particles are usually TiB_2 particles from the Al-5Ti-1B master alloy. Once each nucleation event occurs the growth of this new grain re-establishes sufficient CS to trigger a subsequent nucleation event. This cycle is repeated as a wave of nucleation towards the thermal centre of the casting. Therefore, the grain size can be predicted by understanding the elements that control the distance between each successful nucleation event and this distance equals the grain size.

It was found that there are three critical distances that set the distance between each nucleation event: the distance x_{CS} a new grain grows to generate sufficient CS to cause nucleation (i.e. ΔT_{CS}), the diffusion distance x'_{dl} in front of this grain to the point where ΔT_{CS} equals the nucleation undercooling of the most potent particle (i.e. ΔT_n), and the distance x_{Sd} to the location of the most potent particle. Equation 1 is the Interdependence Model which calculates these three distances allowing prediction of grain size.

$$d_{gs} = x_{cs} + x'_{dl} + x_{Sd} = \frac{D \cdot z \cdot \Delta T_{n-min}}{v \cdot Q} + \frac{4.6 \cdot D}{v}\left(\frac{C_l^* - C_0}{C_l^* \cdot (1-k)}\right) + x_{Sd} \quad (1)$$

where D is the diffusion coefficient, v the rate of growth of the solid-liquid (S-L) interface, C_l* the composition of the liquid at the S-L interface at x_{CS}, $\Delta T_{n\text{-}min}$ the undercooling required for nucleation on the largest and, therefore, most potent available particle, and $z\Delta T_{n\text{-}min}$ is the incremental amount of undercooling required to activate the next nucleation event as the temperature gradient moves towards the thermal centre of the casting. The constant 4.6 is a cut-off factor for the solute profile in front of the S-L interface where $(C_l(x')\text{-}C_o)/(C_l^*\text{-}C_o)$ = 1%.

In a recent paper [9] this equation was simplified to Equation 2 by combining the first two terms in Equation 1 such that

$$d_{gs} = 5.6\left(\frac{D \cdot z\Delta T_n}{v \cdot Q}\right) + x_{sd} \quad (2)$$

Equation 2 highlights the two parameters that dominate the formation of a new grain. The first term describes the Nucleation-Free Zone (NFZ) because no nucleation is possible within this distance because ΔT_{CS} is less than ΔT_n of the most potent particle. The second term represents the distance to an appropriate particle and is controlled by the particle number density provided by the amount of master alloy added.

As shown schematically in Figure 1 both terms make a significant contribution to the final grain size of most alloys [17]. Figure 1 represents the case where the particle number density of TiB_2 particles is constant. This representation is supported by our previous work [3] where the contribution of Ti solute was

determined for a constant TiB_2 particle number density [3]. Figure 2 presents the experimental results for three TiB_2 addition levels.

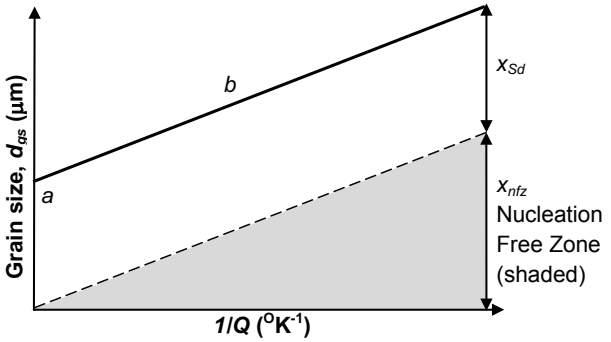

Figure 1. Schematic diagram showing the change in grain size with change in the value of Q for the case where the particle number density remains constant [17].

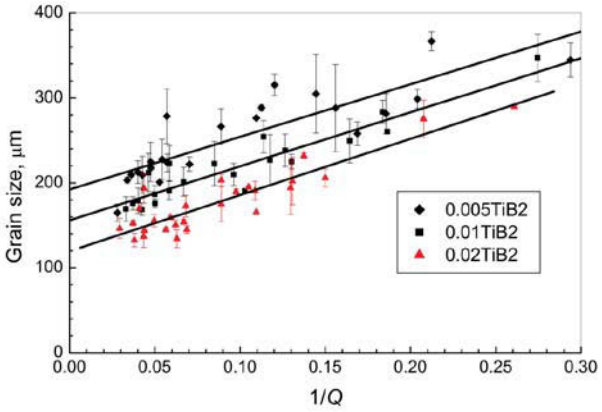

Figure 2. Grain size versus $1/Q$ for a range of Al-Ti based alloys for three TiB_2 levels: 0.005, 0.01 and 0.02wt% TiB_2 (after Ref. [3]). A plot of grain size predicted by Equation 1 is essentially equivalent to the lines of best fit for each level of TiB_2 addition.

However, in the case of the Al-5Ti-1B and Al-3Al-1B master alloys both the amount of solute Ti and the particle number density of TiB_2 particles increases with increasing addition of master alloy. In the section on the Application of the Interdependence Model we will quantify the effect of increasing particle number density along with the simultaneous increase in solute content to determine the relevance of the schematic form given in Figure 1 to this situation.

Validation of the Interdependence Model

The Interdependence Model revealed two important factors affecting grain size. One, in keeping with the predictions of Greer et al. [18-20], is that only the most potent particles will become active nucleants for new grains. The other outcome related to this is that the NFZ prevents nucleation on any particles within the zone and further that the amount of CS between two grains will decrease due to overlapping diffusion fields making the likelihood of further nucleation very low. Both these factors explain the very low efficiency of master alloys where less than 1% of particles are thought to become active [21].

To validate these predictions two approaches have been applied. The first is real-time synchrotron x-ray of the solidification of Al-Si-Ti alloys so that the nucleation events can be observed [22]. Figure 3 captures a typical solidification video frame of a partially solidified Al-4wt%Si-Ti alloy. Observation of the video supports the concept of a wave of nucleation events with little or no additional nucleation occurring between the first nucleated grains.

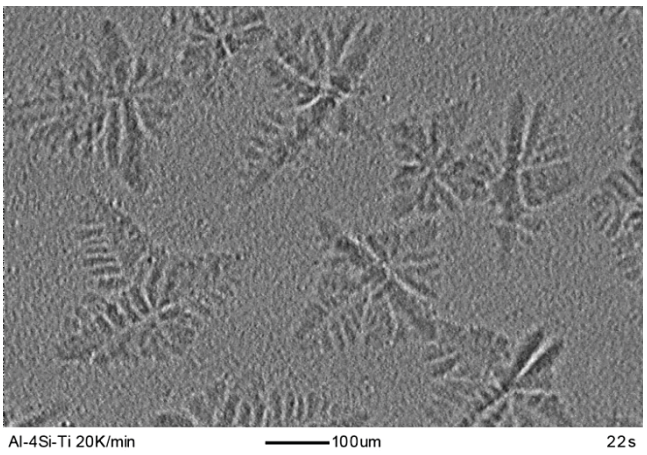

Figure 3. A selected Synchrotron X-ray still of the solidification of the Al-4Si alloy [22].

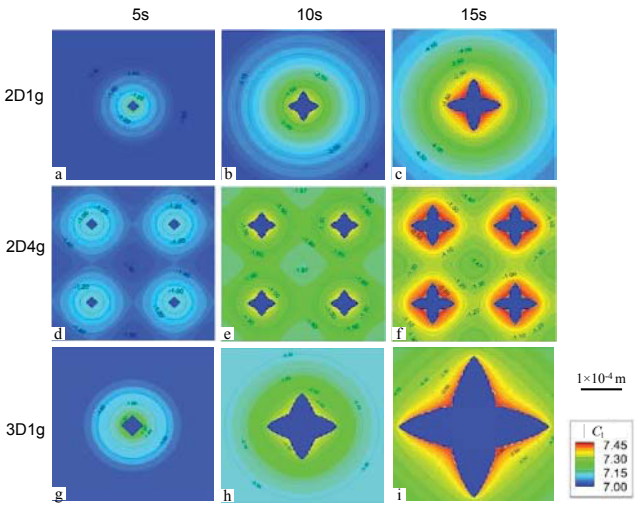

Figure 4. Development of the calculated CS, ΔT_{CS}, with time from μMatIC simulations. The development of ΔT_{CS} after 5s (a,d,g), 10s (b,e,h) and 15s (c,f,i). Isothermal CS contours are shown for different dimensions and the number of grains modeled: 2D1g (a-c), 2D4g (d-f), and 3D1g (g-i) [23].

The second approach is numerical modeling of the formation of the NFZ in 1D, 2D and 3D [23]. Figure **4** is a map of the iso-composition contours between growing grains where the maximum amount of CS is some distance from the solid-liquid interface. The modeling also showed that once the diffusion fields overlap the amount of CS quickly decreases. When overlap begins is dependent on the separation distance between the two grain centers. For larger separation distances a greater amount of CS can be achieved before overlap occurs. If the most potent particles are a long way apart then it is likely that nucleation may occur on one of the next most potent particles that exist between the two grains. Based on these validation studies the Interdependence

Model is a reasonably good embodiment of what is actually occurring during the initial transient of solidification of a casting.

Application of the Interdependence Model

Prediction of the grain size of aluminium alloys

The purpose of this section is to apply the concepts of the nucleation-free zone, x_{nfz}, and the distance to the next particle, x_{Sd}, to data for commercial grain refiners. Currently for wrought alloys there are two main grain refiners: Al-5Ti-1B and Al-3Ti-1B. Al-5Ti-1B is used more commonly whilst Al-3Ti-1B is often used in higher solute situations especially where higher residual Ti contents are present, for example in recycled alloys.

As stated above when grain refining master alloys are added to alloys they typically contain both nucleant particles and solute. However, the Interdependence Model described by Equation 2 has two separate terms where the distance to the nucleant particle and the solute content contribute separately. The empirically derived relationship [3] for an Al-3Ti-1B grain refiner addition to seven different alloys with Ti solute additions up to 0.05wt% is

$$d_{gs} = \frac{652}{Q} + \frac{32}{\sqrt[3]{[TiB_2]}} \qquad (3)$$

Using this equation, grain size calculations were made for various additions of the Al-5Ti-1B and Al-3Ti-1B grain refiners. It was assumed that 2.2% of the Ti in the master alloy combines with the 1%B and the excess Ti (0.8% for the Al-3Ti-1B and 2.8% for the Al-5Ti-1B alloy) is present in the alloy as solute. The addition levels are provided in Table 1 and the grain sizes based on an alloy with a Q-value of 3.1, which is typical of a 1050 alloy (0.3Si, 0.27Fe) are shown in Figure 5. It can be seen that the Al-5Ti-1B master alloy provides better grain refinement than the Al-3Ti-1B alloy for the same addition level. This difference is less evident in alloys with higher Q-values.

Figure 6 plots the three iso-nucleant particle density (dashed) lines from Figure 2 which are straight parallel lines. Two (solid) lines are superimposed on these dashed lines, one of which is related to the addition of Al-5Ti-1B master alloy and the other to Al-3Ti-1B master alloy. The dots on the lines indicate particular grain refinement additions given in Table I. It can be seen that for a particular addition level, the Al-3Ti-1B alloy provides less solute (has a lower Q value or higher $1/Q$). However, for a particular Q-value its grain size is lower because more TiB_2 particles are added for each addition of solute Ti.

Table I. The levels of grain refiner addition that relate to the points on the grain size prediction curves in Figures 5 to 9 for additions of Al-3Ti-1B and Al-5Ti-1B grain refiners.

Addition level (kg/tonne)	Al-3Ti-1B (wt%Ti)	Al-5Ti-1B (wt%Ti)
0.5	0.0015	0.0025
1	0.003	0.005
2	0.006	0.01
5	0.015	0.025
10	0.03	0.05
20	0.06	0.1

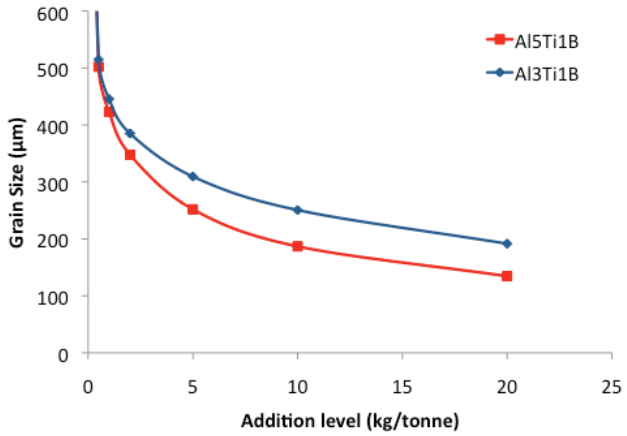

Figure 5. Plot of predicted grain size based on Equation (3) for the addition levels given in Table 1.

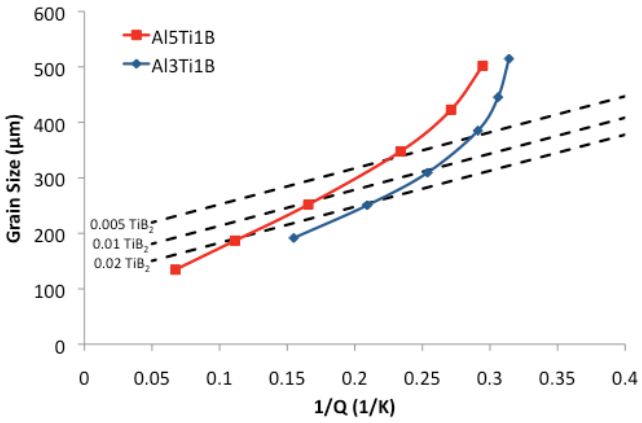

Figure 6. Predictions of grain size for an alloy with a Q value of 3.1 (similar to alloy 1050) given an addition of an Al-5Ti-1B or Al-3Ti-1B master alloy. The dashed lines are from Figure 2 where the TiB_2 content remains constant for each line.

Figure 6 shows that the addition of a master alloy containing both particles and solute is also a relatively straight line but with a slight curve for the low values of Q. Since the grain size is plotted against the inverse of Q, the curve is due to the addition of TiB_2 particles following an inverse cube root relationship with grain size and the reduced effect of Ti solute additions. This relationship means that the change in grain size with each additional increment of TiB_2 particles and Ti solute becomes smaller until each further increment tends towards a straight line as observed in Figure 6. It is clear that the curves in Figure 6 could easily be approximated as a straight line, particularly over a limited range of $1/Q$ values. Further, in the case of the evaluation of experimental data a straight line of best fit could easily be approximated to scattered data therefore concealing the effect of a changing particle number density. This is particularly important when the nucleant particles are introduced by the alloying elements (i.e. native or impurity intermetallic particles), which have not been identified.

Thus, Figure 1 does not represent the situation for master alloys that add both particles and solute. In Figure 7, the data for the Al-5-Ti-1B master alloy is split into the contribution of x_{Sd} and x_{nfz}. It can be noted that, the decrease in x_{Sd} with addition of the Al-

5Ti-1B master alloy contributes as much to the value of the gradient of the grain size plot as the solute does through the gradient of x_{nfz}. For the Al-3Ti-1B master alloy, due to the greater addition of TiB_2 particles at higher addition levels, x_{nfz} is at least an equal contributor to the grain size as x_{Sd}. The values of x_{nfz} are not affected by the TiB_2 content and, therefore, the gradient of x_{nfz} versus $1/Q$ is the same for all plots presented in this paper regardless of the master alloy used. The lines of best fit for the grain size and x_{Sd} for the Al-5Ti-1B master alloy are shown in Table II both for an optimum intercept and for when the line is forced to go through the origin.

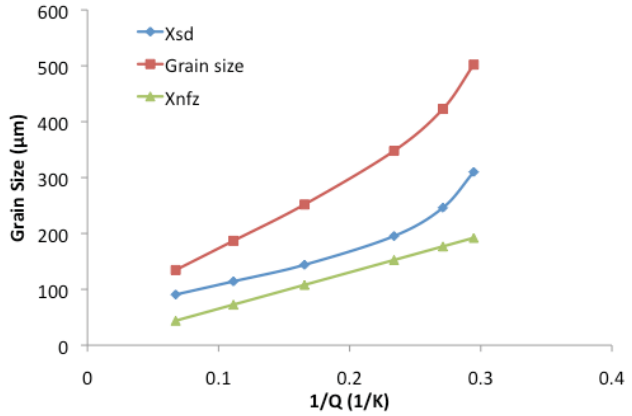

(a)

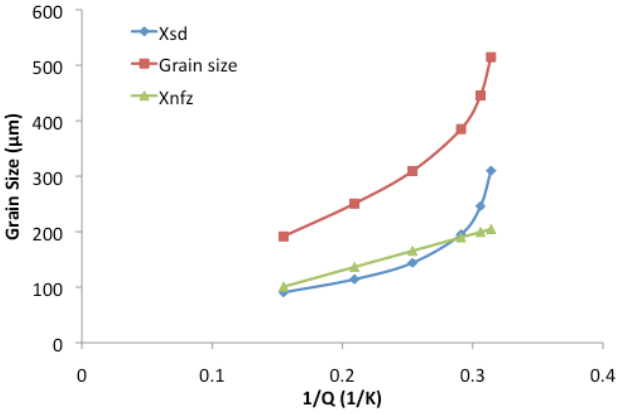

(b)

Figure 7. Contributions of x_{Sd} and x_{nfz} to the grain size on the addition of (a) Al-5Ti-1B and (b) Al-3Ti-1B master alloy to an alloy with a Q value of 3.1., e.g. alloy 1050.

In an alloy with a moderately high solute level with a Q value of 7.8 similar to alloy 6061 (0.52Si, 0.21Cu, 0.05Fe, 0.73Mg), Figure 8 shows that the gradient of the grain size plot is greatly increased because the Ti solute has less of an effect on the grain size because of the higher Q value of the base alloy. It should be pointed out that this Q value is still moderately low compared with Al-Si foundry alloys having Q values close to 50. In this case, there appears to be little benefit in using the Al-5Ti-1B master alloy compared with the Al-3Ti-1B master alloy.

When the grain size is broken into the two components, x_{Sd} and x_{nfz} (Figure 9), it can be clearly seen that the grain size is dominated by x_{Sd}. Hence, in this alloy it is very important to reduce the value of x_{Sd} by adding more TiB_2 particles so that extra nucleation can occur. The lines of best fit for the grain size and x_{Sd} are shown in Table II both for an optimum intercept and for when the line is forced to go through the origin.

It is clear from Figure 7 and Figure 9 that the addition of solute and nucleant particles together leads to a substantial increase in the slope of the curve and a decrease in the intercept with the y-axis compared to when the TiB_2 content is constant (i.e. the dashed lines). Both these changes were observed for the addition of Zr master alloy to magnesium where Zr provides both growth restricting solute and potent particles [24]. This may be part of the reason why in some systems very low or negative intercepts are observed as is observed by the lines of best fit for this data (Table II) (although if the particles are unknown it may be difficult to separate this effect from a situation where there are a large number of relatively poor nuclei).

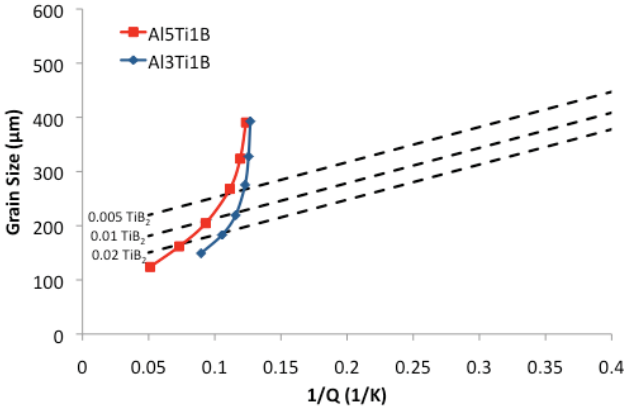

Figure 8. Predictions of grain size for an alloy with a Q value of 7.8 (similar to alloy 6061) given an addition of an Al-5Ti-1B or Al-3Ti-1B master alloy.

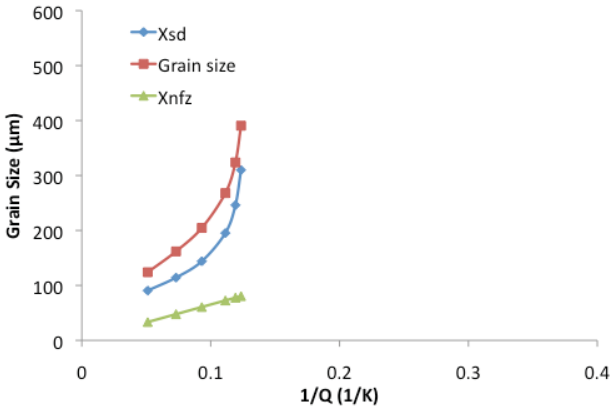

Figure 9. Contributions of x_{Sd} and x_{nfz} to the grain size on the addition of Al-5Ti-1B alloy to an alloy with a Q value of 7.8, e.g. 6061.

By comparing Figures 7(a) and 9 it easy to observe the relative impact of master alloy additions on the grain size for the two cases of low and high Q-values for typical aluminium alloys. For the low Q-value case, both the solute and particles make a similar contribution to reducing the grain size. That is, as solute from the master alloy is added (i.e. $1/Q$ decreases) the grain size decreases while the grain size also drops across the dashed lines showing

that the additional TiB_2 particles are also decreasing the grain size. For the high Q-value alloy the grain size initially drops quickly across the dashed lines indicating that the addition of TiB_2 particles is making the strongest contribution to the grain size. This observation suggests that the addition of Al-5Ti-1B is most suitable for low Q-value alloys and that Al-3Ti-1B is adequate for refining high Q-value alloys, which is how the master alloys are often used in practice.

Table II. Data for the lines of best fit in Figure 7(a) and Figure 9.

	Gradient (μm/K)	Intercept (μm)	R^2
Q=3.1 Grain size	1539.3	14.0	0.97
	1601.9	0	0.97
Q=3.1 x_{Sd}	887.3	14.2	0.92
	850.0	0	0.92
Q=7.8 Grain size	3345.6	-73.2	0.89
	2630.4	0	0.85
Q=7.8 x_{Sd}	2693.6	-73.2	0.84
	1978.4	0	0.78

Based on the above, Figure 1 can be adjusted to take into account the simultaneous increase in particle number density as illustrated in Figure 10.

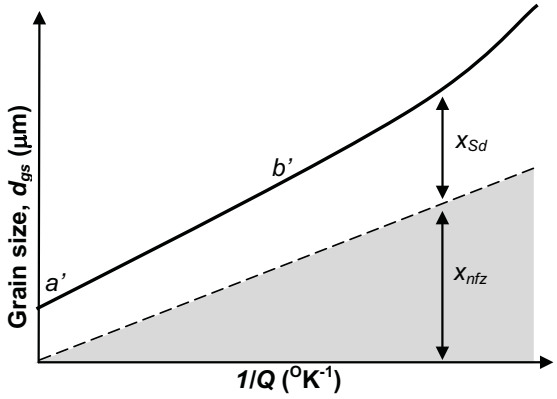

Figure 10. Schematic diagram showing the change in grain size with change in the value of Q for the case where the particle number density increases with increase in solute content.

Calculation of x_{Sd}

The above analysis highlights the important effect particle number density has on x_{Sd} and, therefore, grain size. Figure 11 shows the potency distributions against the average distance to the corresponding particle, ΔT_n-S_d, for each of the three experimental densities of TiB_2 particles obtained from the Al-5Ti-1B master alloy used to develop Figure 2 [3]. The values of x_{Sd} measured at the intercept in Figure 2 range from 190 μm to 120 μm for the 0.005%TiB_2 and the 0.02%TiB_2 additions respectively [3], and, as illustrated by the dashed line in Figure 11, correspond to ΔT_n of approximately 0.2 - 0.25 °C. These values compare well with reports from the literature [19]. ΔT_n in the range 0.2 - 0.25 °C corresponds to a particle diameter of about 2.5 μm representing about 1.8% of the added particles [19]. This percentage is similar to the previous estimates in the range of 1-2% [21]. At a $1/Q$ value of 0.3 (Q~3.1) for the 0.005%TiB_2 addition, the grain size is approximately 375 μm suggesting that about 0.3% of the particles are active. This observation indicates that the nucleation-free zone can reduce the number of active particles by 80% or more in lean alloys. This effect of NFZ implies that even a grain refiner with a very narrow size range of potent (i.e. large) nucleant particles would not be able to obtain very high nucleation efficiencies, particularly in lean (i.e. low Q value) alloys.

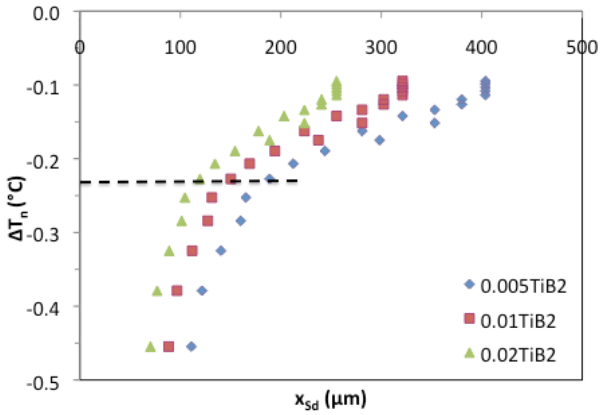

Figure 11. ΔT_n against x_{Sd} for the range of particle diameters for 0.005%, 0.01% and 0.02% additions of TiB_2 particles provided by an Al-5Ti-1B master alloy [25].

Using the same methodology as in Ref. [24]

$$x_{Sd} = \frac{1000}{\sqrt[3]{\frac{TiB2_A}{TiB2_{MA}} . N_{v(d_{Pi} \le d_p \le d_{Pj})}}} \quad (4)$$

where $TiB2_A$ is the amount of TiB_2 added, $TiB2_{MA}$ is the weight percent of TiB_2 in the master alloy, N_v is number density of TiB_2 particles in the Al-5Ti-1B master alloy that are able to become active and which are defined by the size range between d_{Pi} and d_{Pj} (in μm). Based on the analysis of Figure 11 the range of d_{Pi} is 2.5±0.25μm. Empirical relationships for this term for the alloys evaluated here can be found in Table II.

Prediction of grain size refined by Al-Ti-B master alloys

Considering the above analysis we are able to develop an equation that predicts the grain size for the casting conditions used for this work

$$d_{gs} = 5.6\left(\frac{D.z\Delta T_n}{v.Q}\right) + \frac{1000}{\sqrt[3]{\frac{TiB2_A}{TiB2_{MA}} . N_{v(d_{Pi} \le d_p \le d_{Pj})}}} \quad (5)$$

The main consideration for the addition of grain refiners, such as Al-5Ti-1B is that they contribute both to the nucleant particle density and the solute content. Replacing the first term in Equation 5 with the first term in Equation 3 (625/Q) and defining d_{Pi} as 2.5 μm gives Equation 6 for the solidification conditions used to generate Figure 2:

$$d_{gs} = \frac{652}{Q_{alloy} + Q_{gr}} + \frac{1000}{\sqrt[3]{\frac{TiB2_A}{TiB2_{MA}} . N_{d\sim 2.5\mu m}}} \quad (6)$$

To develop a similar equation for the Al-3Ti-1B master alloy requires the measurement of the particle size distribution as has been done for the Al-5Ti-1B master alloy [19]. By using the composition of the base alloy and the Ti solute added by the master alloy (Table 1) the value of Q can be calculated and inserted into Equation 6. The value of $TiB2_A$ can also be taken from Table 1. The value of N_v is the total TiB_2 particle content of the master alloy for the range of particle sizes that can be activated (Figure 11).

This work has clearly shown the relative contributions of solute Ti and TiB_2 particles to the grain size. Equation 6 has quantified these contributions for the Al-5Ti-1B master alloy and a similar equation could be developed when the TiB_2 particle size distribution for the Al-3Ti-1B master alloy is measured. In future work we will verify this analysis and the predictive equations for common alloy systems such as Al-Si alloys.

Conclusions

The Interdependence Model provides a useful basis on which to analyse the performance of master alloys. This analysis has shown that the roles of solute and particles provided by Al-Ti-B master alloys are both important factors in controlling grain size. A predictive equation based on these two contributions has been developed for the determination of grain size for the casting conditions used for the acquisition of grain size data. For lean low Q-value alloys both solute and particles make approximately equal contributions to the final grain size indicating that the Al-5Ti-1B master alloy is the best choice for these alloys. For alloys with higher base Q-values the addition of TiB_2 particles makes a greater contribution to achieving the desired grain size and thus the Al-3Ti-1B master alloy will achieve a suitable degree of refinement.

Acknowledgements

Support was provided by the CAST CRC, ARC Discovery Grants DP2010000071 (ME) and DP120101672 (DStJ, AP), and the Centre for Advanced Materials Processing and Manufacturing (AMPAM) at UQ (DStJ, AP).

References

[1] Easton MA, StJohn DH. 4th Asian Foundry Congress. Gold Coast, Australia, 1996. p.407.
[2] Easton MA, StJohn DH. Mater. Sci. Engng. A 2008;486:8.
[3] Easton MA, StJohn DH. Metall. Mater. Trans. A 2005;36A:1911.
[4] Easton MA, StJohn DH. Acta Mater. 2001;49:1867.
[5] Easton MA, StJohn DH. Metall. Mater. Trans. A 1999;30A:1613.
[6] Easton MA, StJohn DH. Metall. Mater. Trans. A 1999;30A:1625.
[7] Cao P, Qian M, StJohn DH. Scripta Mater. 2007;56:633.
[8] Qian M, Ramirez A, Das A, StJohn DH. J. Cryst. Growth 2010;312:2267.
[9] StJohn DH, Easton MA, Qian M, Taylor JA. Metall. Mater. Trans. A 2013;44:2935.
[10] StJohn DH, Qian M, Easton MA, Cao P, Hildebrand Z. Metall. Mater. Trans. A 2005;36A:1669.
[11] StJohn DH, Cao P, Qian M, Easton MA. Adv. Engng. Mater. 2007;9:739.
[12] Bermingham MJ, McDonald SD, StJohn DH, Dargusch MS. Philos. Mag. 2010;90:699
[13] Bermingham MJ, McDonald SD, Nogita K, St. John DH, Dargusch MS. Scr. Mater. 2008;59:538.
[14] Bermingham MJ, McDonald SD, Dargusch MS, St. John DH. Scr. Mater. 2008;58:1050
[15] StJohn DH, Qian M, Easton MA, Cao P. Acta Mater. 2011;59:4907.
[16] Qian M, Cao P, Easton MA, McDonald SD, StJohn DH. Acta Mater. 2010;58:3262.
[17] StJohn DH, Easton MA, Qian M, Cao P, Bermingham MJ. In: Fan Z, Stone IC, editors. Proceedings of the John Hunt Symposium. Brunel University: Brunel University Press, London, UK, 2011. p.45.
[18] Tronche A, Greer AL. Phil. Magos. Lett. 2001;81:321.
[19] Quested TE, Greer AL. Acta Mater. 2004;52:3859.
[20] Greer AL, Bunn AM, Tronche A, Evans PV, Bristow DJ. Acta Mater. 2000;48:2823.
[21] Perepezko JH. Metals Handbook, vol. 15. Metals park: ASM, 1988. p.101.
[22] Nogita K, H Y, Prasad A, McDonald SD, Nagira T, Nakatsuka N, Uesugi K, StJohn DH. Mater. Char. 2013:accepted for publication 28 August 2013.
[23] Prasad A, Yuan L, Lee PD, StJohn DH. Acta Mater. 2013;61:5914.
[24] Sun M, Easton MA, StJohn DH, Wu G, Abbott TB, Ding W. Adv. Engng. Mater. 2012;15:373.
[25] StJohn DH, Easton MA, Qian M. In: Wetland H, Rollett AD, Cassada WA, editors. 13th International Conference on Aluminum Alloys. Pittsburg, PA: TMS (The Minerals, Metals & Materials Society), 2012. p.1419.